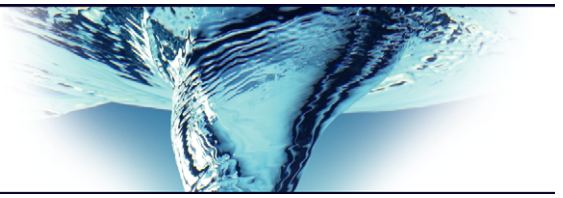
J. Fluid Mech. (2013), *vol.* 734, R2, doi:10.1017/jfm.2013.475



JFM RAPIDS
journals.cambridge.org/rapids

Mixing in gravity currents

A. T. Fragoso[1,†], M. D. Patterson[2] and J. S. Wettlaufer[1,3]

[1]Yale University, New Haven, CT 06520-8109, USA
[2]University of Bristol, University Walk, Bristol BS8 1TR, UK
[3]Mathematical Institute, University of Oxford, Oxford OX2 6GG, UK

(Received 10 July 2013; revised 6 September 2013; accepted 9 September 2013;
first published online 8 October 2013)

We study entrainment in lock-release gravity currents using highly spatially resolved optical transmission experiments and quantitative analysis of the available potential energy of the flow. The principal results provide a resolution to the debate regarding the mechanism and degree of mixing in the head of a gravity current during the slumping phase. The nature of the complex internal mixing structure changes as a bore propagates from the tail to the head of the current during the slumping phase and overtakes its leading edge. We use quantitative methods to identify the connection between dynamics and entrainment and show that its manifestation as examined using different methodologies is the cause of previous contradictory experimental findings. Therefore, we conclude that the two main perspectives previously considered at odds are in accord.

Key words: gravity currents, turbulent mixing

1. Introduction

Gravity currents are fluid flows driven by density differences. In the atmosphere, lakes, seas and oceans the density differences can be caused by variations in salinity, temperature or the concentration of suspended particulates. The principal laboratory model is the instantaneous release of a fixed volume of dense fluid into a much larger volume of lighter fluid by removal of a partition. It is widely accepted that the large-scale dynamic behaviour of these flows is well explained by relatively simple box models and by shallow-water theory (e.g. Hoult 1972; Huppert & Simpson 1980). These approaches are robust and accurately describe the front speed and height of the flow, but they do not provide spatio-temporal information regarding the entrainment of ambient fluid into the head of the current during propagation. Consequently, attempts to experimentally determine the nature of mixing in this regime have produced what

† Present address: California Institute of Technology, Mail Code 105-50, Pasadena, CA 91125, USA. Email address for correspondence: afragoso@caltech.edu

© Cambridge University Press 2013

https://doi.org/10.1017/jfm.2013.475 Published online by Cambridge University Press

have been considered to be contradictory results. Here, we demonstrate that two perspectives previously considered at odds are in fact in accord.

By following an alkaline current into an acidic ambient, Hallworth *et al.* (1993, 1996) investigated entrainment phenomena theoretically and experimentally using a coloured pH indicator for visual observation. As the head propagated forward, they observed that entrainment took place almost entirely at the head of the current by: (*a*) Kelvin–Helmholtz instabilities at the interface between the current and the ambient; and (*b*) the over-riding of the less-dense ambient fluid trapped at the no-slip lower boundary (see e.g. Simpson 1972). Entrainment into the head of the current was not observed until the end of the slumping phase, which is defined as the time required for a bore to travel backwards from the front of the current, reflect off the back wall, and catch up with the head (Rottman & Simpson 1983; Bonnecaze, Huppert & Lister 1993). During this period the current head propagates at an approximately constant velocity and travels a distance x_s to the *slumping point* (Rottman & Simpson 1983). After passing the slumping point, the velocity of the current satisfies a similarity solution; it is at that point that Hallworth *et al.* (1993, 1996) began to observe dilution of the head. They noted that although they could provide no physical explanation for the apparent connection between this transition and entrainment into the head, their observations were consistent with this scenario.

Hacker, Linden & Dalziel (1996) presented results from three experiments using the attenuation of transmitted light by dye as a measure of mixing. The spatial and temporal variations of the transmitted intensity through the head of the gravity current correspond to variations in dye concentration, which in turn correspond to variations in density. These experiments, although limited in range and number, revealed a complex internal density structure with mixing occurring almost immediately after collapse. When characterizing the discrepancy between this result and that of Hallworth *et al.* (1993, 1996), Huppert (2006) summarized that 'A resolution of these different conclusions is awaited'.

Here, we resolve this discrepancy quantitatively and link dynamics predicted by shallow-water theory to entrainment during the slumping phase. While our experimental technique (§ 2) follows the basic method proposed by Hacker *et al.* (1996), technical advances provide us with a much finer view of the mixing and slumping processes and the interpretation is made substantially richer by an application of the available potential energy (APE) framework developed by Winters *et al.* (1995). This approach was also used by Patterson *et al.* (2006) to examine mixing caused by turbulent instabilities of Kelvin–Helmholtz billows in two-layer stratified shear flows.

2. Experimental methods

As is standard in laboratory investigations of gravity current behaviour, a dense solution, here made from sugar and water, was placed behind a plastic lock in a 2.4 m × 0.5 m × 0.1 m tank filled with tap water (figure 1). Experiments were performed at a variety of reduced gravities ($g' = g(\rho_{current} - \rho_{ambient})/\rho_{ambient}$, where g is the acceleration due to gravity, and $\rho_{current}$ and $\rho_{ambient}$ the relevant fluid densities), aspect ratios (defined as the initial ratio of current height to length), and fractional depths (defined as the initial ratio of current height to ambient height), see table 1. In order to construct a stratified configuration for several of the experiments, ambient fluid was carefully floated over the dense solution to create starting geometries at fractional depth less than unity. A uniform LED backlight was placed behind the tank,

https://doi.org/10.1017/jfm.2013.475 Published online by Cambridge University Press

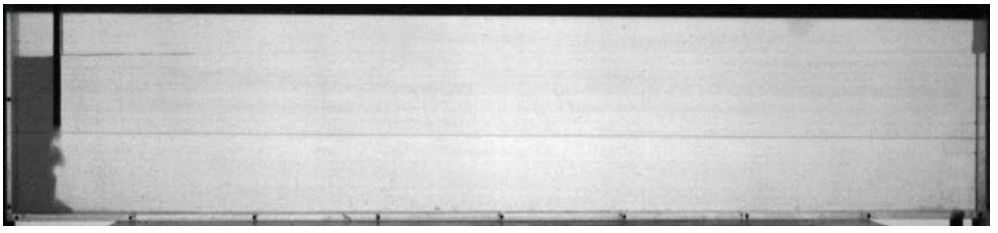


FIGURE 1. Picture of our apparatus which uses the canonical setup for lock-release gravity currents. Our tank is 2.4 m long, 0.5 m tall and 0.1 m wide and we remove a plastic lock (dark vertical line on the left-hand side) to release a dyed sugar solution (dark fluid, left-hand side) into a tap water ambient (majority of the field of view here). An LED backlight illuminated the current, which allowed light attenuation to be measured by a camera and converted into a density map by a calibration curve.

Exp. no. (trials)	Aspect ratio	Fractional depth	g'
1 (3)	0.5	1	12
2 (3)	1.5	1	12
3 (3)	2.5	1	12
4 (4)	0.5	0.67	12
5 (4)	0.5	0.33	12
6 (3)	1	1	12
7 (4)	1	1	24
8 (4)	1	1	36

TABLE 1. Experiments were conducted across a large range of initial geometries and reduced gravities. The first column denotes the experiment number shown in this paper and in parentheses the number of experimental runs for varying aspect ratio, fractional depth and reduced gravity g'. Movies of these currents are provided in the online supplementary information (available at http://dx.doi.org/10.1017/jfm.2013.475). In addition to the experiments presented, 67 other trials were performed at intermediate initial conditions. The Reynolds number is of order 10^3, and the Schmidt number ν/D, where ν is the kinematic viscosity of water and D is the diffusion coefficient of sugar, is of order 10^4.

and a known concentration of red dye was added to the sugar–water solution as a tracer. The lock was removed abruptly, and an approximately two-dimensional gravity current propagated down the tank and was captured by a digital camera (Dalsa 4M60 at 10 f.p.s.) connected to a computer.

Under an imaging scheme similar to that of Hacker *et al.* (1996) and Patterson *et al.* (2006), the camera recorded light attenuation due to the presence of dye in dense regions of the current. These images were captured with the visualization program Digiflow and subsequently transferred to Matlab for processing. With the intensity of each pixel in control conditions, i_0, and its intensity in experimental conditions, i, both known, a light attenuation value i/i_0 was assigned to each pixel for each frame. The dye concentration at each point in the tank was then calculated through an experimentally determined calibration curve that related recorded light attenuation to an actual dye concentration. Because tracer dye was initially restricted to the

https://doi.org/10.1017/jfm.2013.475 Published online by Cambridge University Press

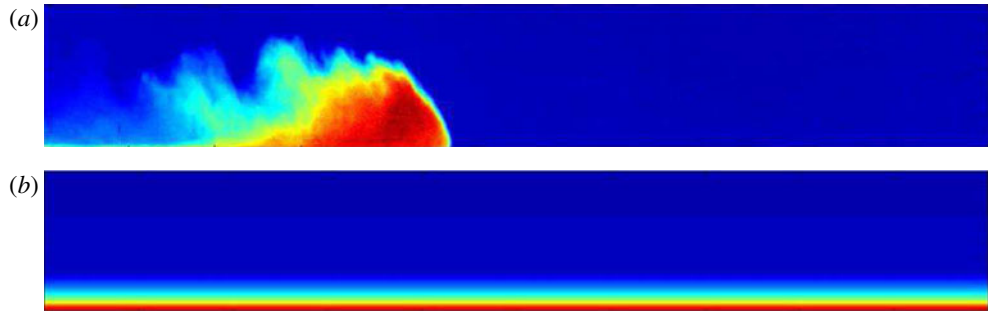


FIGURE 2. An experimental density distribution of fluid elements (*a*) is transformed adiabatically to an energetic minimum (*b*) using the framework developed by Winters *et al.* (1995) and outlined in our § 2.

initial dense core of the current, the generation of dilute regions of dye concentration can be directly attributed to irreversible mixing. Accordingly, a density map can be determined from the ratio of dye concentration at each point to the original maximum concentration in the current and the densities of the background and the initial dense solution. Because the camera cannot distinguish three-dimensional structure in a current that is only approximately two-dimensional, the light attenuation images record spanwise-average values.

Although the LED strip was spatially uniform, signal noise in the light attenuation images was introduced by the unfiltered fluctuations from a standard AC electrical outlet. Following Jackson (2010), in order to filter this noise, a region of the active experimental tank that did not encounter dye was selected as a control. Through addition or subtraction at each pixel value, the control area was fixed to a constant brightness level equal to its average. By extension to the entire tank, transient noise was filtered to a magnitude below camera resolution.

After conversion of the image to a matrix of pixel values, previously unavailable quantitative analysis of the internal structure and evolution of the current was performed. The precision afforded provides a new perspective of the current evolution.

The contribution of large-scale reversible 'stirring' was distinguished from the irreversible 'mixing' of fluid elements using the physical and mathematical framework of Winters *et al.* (1995). This approach explicitly partitions the changes in potential energy due to adiabatic processes, which advect fluid elements without molecular mass or heat transfer, from changes due to diabatic processes that tend to dilute dense fluid elements. The background potential energy E_b is defined as the minimum potential energy attainable through an adiabatic redistribution of the density field (figure 2). Thus, for an experimental density field $\rho(x, z, t)$, where x is the horizontal coordinate, z is the vertical (positive up) coordinate, and t is time, the total potential energy is

$$E_p(t) = g \int_V \rho(x, z, t) z \, \mathrm{d}V, \tag{2.1}$$

and the background potential energy of a rearranged density field $\rho^*(x, z, t)$ is

$$E_b(t) = g \int_V \rho^*(x, z, t) z \, \mathrm{d}V, \tag{2.2}$$

https://doi.org/10.1017/jfm.2013.475 Published online by Cambridge University Press

where both integrals are taken over the volume of the tank V. These values are acquired experimentally by sampling the density field with a camera and performing the integral numerically after image processing. As a result, the background state depends only on the probability density function of the density field over the ensemble of fluid parcels, and is independent of their spatial distribution. Adiabatic processes can only result in a spatial redistribution of the density field and associated changes in the total potential energy E_p, but cannot alter the background state. Therefore, the two regimes of potential energy discharge can be separated in a robust time-dependent manner: the extent of mixing due to dilution can be directly tracked through E_b, while the reversible conversion of potential energy into kinetic energy is tracked through the available potential energy $E_a = E_p - E_b$. The isolation of these components is an essential part of our analysis.

3. Results

Figure 3 shows the evolution of the spanwise-averaged density field for a representative experiment before the slumping point, divided into relatively coarse contours to aid visualization. Immediately after collapse, a large Kelvin–Helmholtz billow forms behind the head of the current and is ultimately involved in mixing dense fluid from the head with fluid from the ambient. Mixing also occurs by a lobe-and-cleft interaction at the head of the current as an intrusion of lighter fluid underneath the dense head, visible in figure 3(*b*), as well as by smaller Kelvin–Helmholtz billows that form at the front and interact with dense fluid drawn up by the large billow at the rear as they propagate towards the back. The expansion of less-dense contours at the expense of denser contours is also readily apparent. For a variety of initial conditions figure 4 details the size of the region with density greater than each threshold value from figure 3, each of which produces a clear increase in the size of lighter contours at the expense of denser contours. We also provide an analysis of the energetics for the same series of experiments in figure 5. Clearly, figure 4 shows that both the magnitude and the time evolution of the mixing depend on the density resolution threshold used. Thus, on the one hand, if mixing were to begin at the slumping point, a distinct change in the fractional area of the current would be seen and a corresponding increase in the production of dilute fluid elements would manifest itself as a sudden increase in the adiabatically rearranged potential energy. For the entire range of experiments shown in table 1, we observe no such abrupt events. On the other hand, in figure 6 and the movies provided in the online supplementary material, we show an example of how the current decelerates from the constant speed regime into the self-similar regime as a reflected return flow – the bore – overtakes the head of the current, extinguishes the large billow behind the head, and thereby abruptly suppresses/eliminates mixing there. This finding is consistent with the slumping mechanism reported by Rottman & Simpson (1983) and used by Hallworth *et al.* (1993, 1996) in the interpretation of their pH indicator experiments. We also observe that mixing ultimately caused by the billow is internal to the current and difficult to identify without the aid of the full density field.

Because the method of Hallworth *et al.* (1993, 1996) only distinguishes the homogeneous current head from the diffuse wake of undetermined density, it effectively shields the entrainment coefficient defined therein from the consequences of the complex internal density structure of the head. Comparison between the visual assessment of mixing (figure 4) and the energetics (figure 5), demonstrates that while different choices of the threshold between 'head' and 'diffuse wake' can produce

https://doi.org/10.1017/jfm.2013.475 Published online by Cambridge University Press

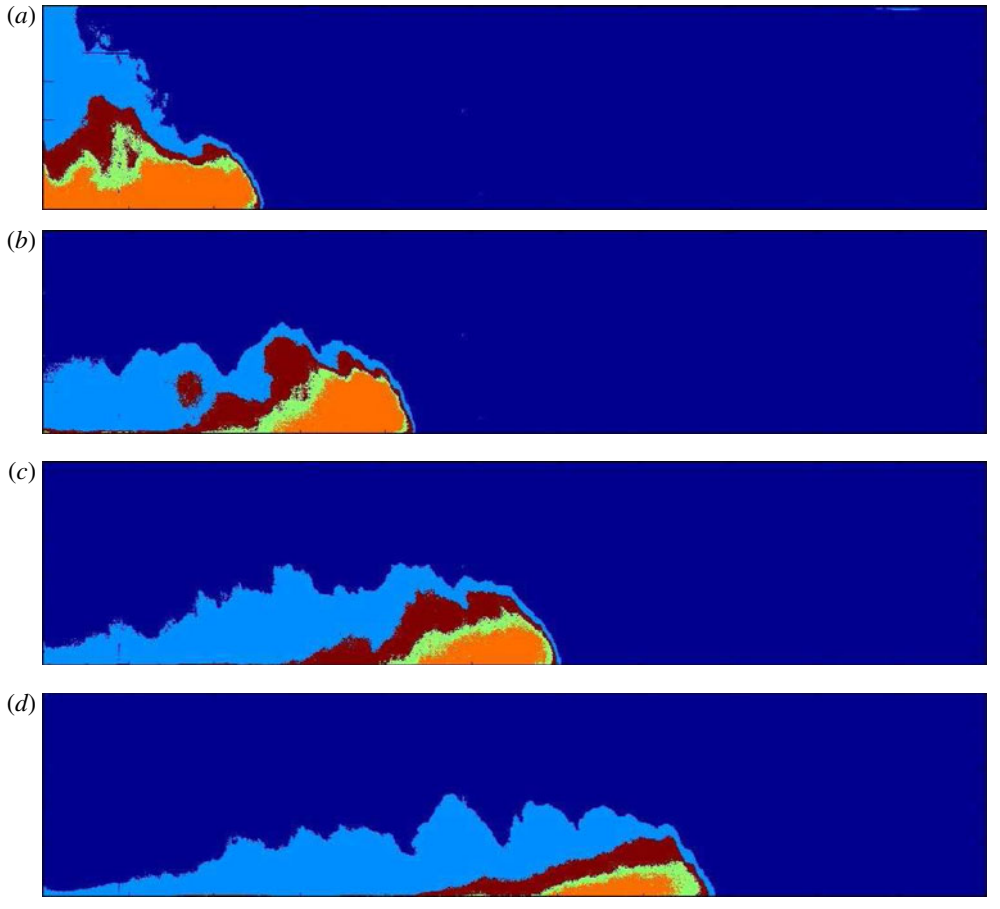


FIGURE 3. A density contour map of a typical gravity current over time, with the slumping point reached in the last frame, (*d*). Thresholds mark percentages of the density difference between the original current and the ambient: the dark blue region is at ambient density, light blue exceeds ambient density by the margin of error of the camera (0.0003 g ml^{-1}), red exceeds 50 % of the density difference, green exceeds 80 %, and orange exceeds 92 %. The dense regions of the current decrease significantly in size as they lose material to dilution due to a complex internal structure. Here, the initial aspect ratio is 1.5, $g' = 12$, and fractional depth is 1.

different physical interpretations for irreversible mixing, the energetics show that it is independent of that choice. This suggests that observed correlation between entrainment and the slumping distance is associated with the thresholding of density. Due to the fact that the internal mixing structure in the head observed here and by Hacker *et al.* (1996) is eliminated by the bore propagation during the slumping mechanism, we believe that Hallworth *et al.* (1993, 1996) only begin to observe intrusion of ambient fluid, to which their method is sensitive, once internal mixing no longer plays a dominant role, namely after the slumping point. For this reason, accurate measurement of mixing in the current cannot rely on density threshold methods alone and must include an integral method, such as rearranged potential energy, to characterize the evolution of a continuous density field.

https://doi.org/10.1017/jfm.2013.475 Published online by Cambridge University Press

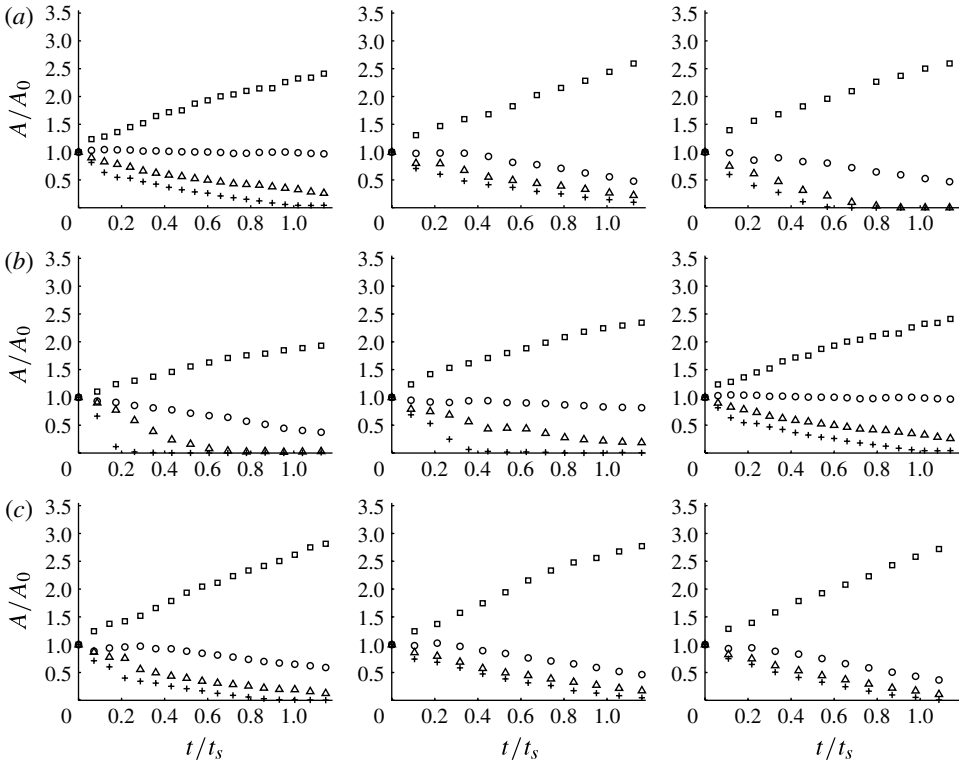


FIGURE 4. The area of the current greater than each of the thresholds from figure 3, plotted as a function of time for a variety of initial conditions: □, exceeds ambient density by the margin of error of the camera (0.0003 g ml^{-1}); ○, 50 %; △, 80 % and +, 92 %. Here, area A is scaled by the initial area of each threshold A_0 and time is scaled by the time required to reach the slumping distance t_s. (*a*) Fractional depth = 1 and reduced gravity = 12 held constant, and aspect ratios (from left) 0.5, 1.5 and 2.5. (*b*) Aspect ratio = 0.5 and reduced gravity = 12 held constant, and fractional depths (from left) 0.33, 0.67 and 1. (*c*) Aspect ratio = 1 and fractional depth = 1 held constant, and reduced gravities (from left) 12, 24 and 36. Clearly, both the magnitude and the time evolution of mixing observed depends on the resolution threshold chosen.

4. Conclusion

We have performed a wide range of lock-release experiments and find significant entrainment and mixing within the dense core of gravity currents throughout the slumping phase. The experimental method resolves the debate over the extent of mixing that occurs during this time, which is shown to depend on how precisely the density field is sampled. Whereas the limited range of experiments performed by Hacker *et al.* (1996) showed immediate mixing after collapse using an early version of the light attenuation method we employ, Hallworth *et al.* (1993, 1996) reached 'a particularly surprising result' in their observation that 'the head remains essentially unmixed – the entrainment is negligible – in the slumping phase' when a visual pH colour threshold method was used to monitor entrainment. Our highly resolved light attenuation experiments show both behaviours to be operative. At the finest resolutions we see mixing occur at the initial stages of release, the formation

https://doi.org/10.1017/jfm.2013.475 Published online by Cambridge University Press

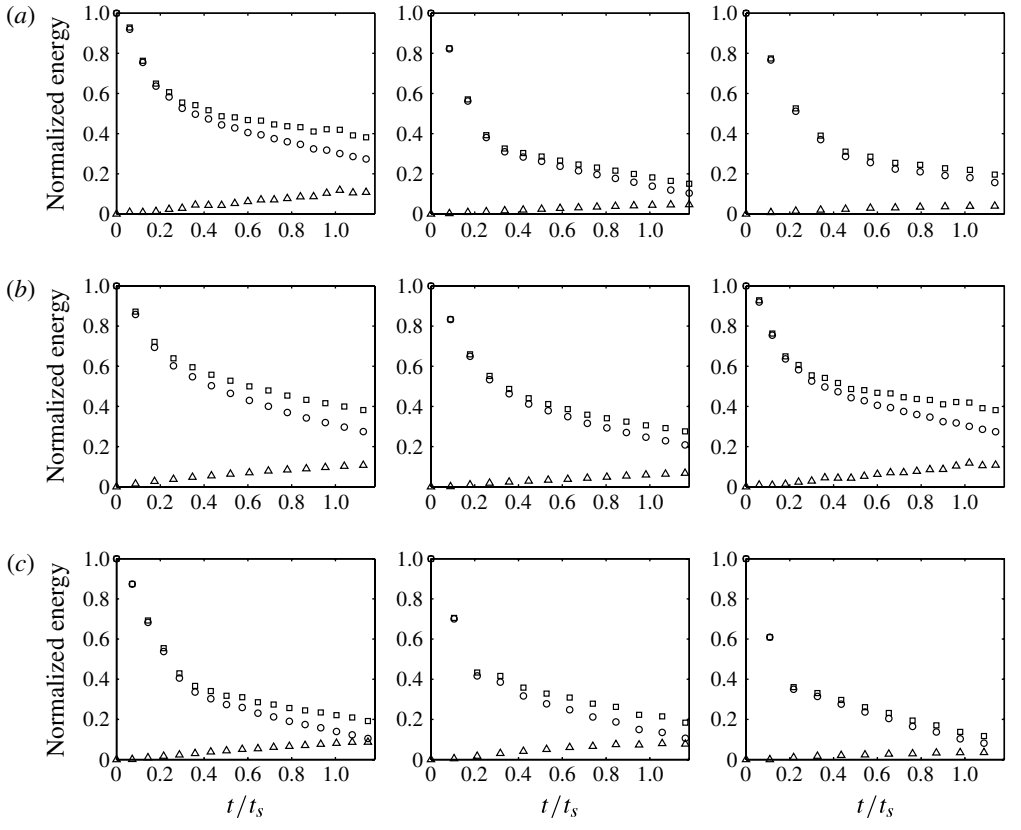


FIGURE 5. Energetics plots for the suite of experiments shown in figure 4. Here, □ is total potential energy E_p, △ is the adiabatically rearranged background potential energy E_b, and ○ is the difference between the two. Energy is normalized so that the minimum $E_b = 0$ and the maximum $E_p = 1$, and time is scaled by the time required to reach the slumping distance t_s. A sudden irreversible mixing event would appear as a sharp increase in E_b, and is not observed over a wide range of initial conditions. (*a*) Aspect ratios (from left) 0.5, 1.5 and 2.5; (*b*) fractional depths (from left) 0.33, 0.67 and 1; (*c*) reduced gravities (from left) 12, 24 and 36.

and propagation of a bore at the current/ambient interface (which characterizes the upper diluted tail region of the current) and its eventual overtaking of the head of the current to extinguish internal mixing behind it. As indicated by the fractional area of the current, figure 4 shows clearly that one may find a resolution-dependent abrupt change in mixing in the vicinity of the slumping point by choice of threshold. However, this effect disappears as the resolution increases, exhibiting a continuous evolution that is also seen in the overall energetics of the current shown in figure 5. The slumping mechanism is an important process in determining the internal density structure until $t \sim t_s$, after which Kelvin–Helmholtz billows at the front of the current and further over-riding of the ambient dominate entrainment into the head of the current with a visibility that is dependent on the density resolution. Therefore, both views described by Huppert (2006) coexist during the evolution of a current, with one mixing mechanism dominating during the slumping phase and the other afterwards.

https://doi.org/10.1017/jfm.2013.475 Published online by Cambridge University Press

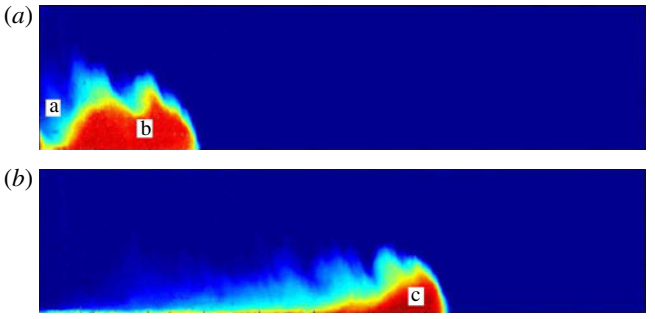


FIGURE 6. The reflected return flow (a) advances along the current until it extinguishes the Kelvin–Helmholtz billow (b) behind the head of the current at the slumping point (c). This mechanism controls the the dynamics of the current but is also an important source of mixing in the head of the current.

Acknowledgements

A.T.F. acknowledges the Yale College Dean's Office, the K. L. Von Damm Research Fellowship, and Connecticut Space Grant Consortium for support of this research and J.S.W. thanks the John Simon Guggenheim Foundation, the Swedish Research Council and a Royal Society Wolfson Research Merit Award for support. J.S.W. is grateful to H. E. Huppert, J. A. Neufeld and M.-L. Timmermans for discussions and feedback at various stages of this work. Early versions of these experiments were the basis of the Yale B.S. theses of R. Berkowitz and R. Jackson. We appreciate having learned from attempts to refine their work.

Supplementary movies

Supplementary movies are available at http://dx.doi.org/10.1017/jfm.2013.475.

References

BONNECAZE, R. T., HUPPERT, H. E. & LISTER, J. R. 1993 Particle-driven gravity currents. *J. Fluid Mech.* **250**, 339–369.

HACKER, J., LINDEN, P. F. & DALZIEL, S. B. 1996 Mixing in lock-release gravity currents. *Dyn. Atmos. Oceans* **24**, 183–195.

HALLWORTH, M. A., HUPPERT, H. E., PHILLIPS, J. C. & SPARKS, R. S. J. 1996 Entrainment into two-dimensional and axisymmetric turbulent gravity currents. *J. Fluid Mech.* **308**, 289–311.

HALLWORTH, M. A., PHILLIPS, J. C., HUPPERT, H. E. & SPARKS, R. S. J. 1993 Entrainment in turbulent gravity currents. *Nature* **362**, 829–831.

HOULT, D. P. 1972 Oil spreading on the sea. *Annu. Rev. Fluid Mech.* **4**, 341–368.

HUPPERT, H. E. 2006 Gravity currents: a personal perspective. *J. Fluid Mech.* **255**, 299–332.

HUPPERT, H. E. & SIMPSON, J. E. 1980 The slumping of gravity currents. *J. Fluid Mech.* **99**, 785–799.

JACKSON, R. 2010 Entrainment in turbulent gravity currents. B.S. Thesis, Yale University.

PATTERSON, M. D., CAULFIELD, C. P., MCELWAINE, J. N. & DALZIEL, S. B. 2006 Time-dependent mixing in stratified Kelvin–Helmholtz billows: experimental observations. *Geophys. Res. Lett.* **33**, L15608.

ROTTMAN, J. W. & SIMPSON, J. E. 1983 Gravity currents produced by instantaneous releases of a heavy fluid in a rectangular channel. *J. Fluid Mech.* **135**, 95–110.

https://doi.org/10.1017/jfm.2013.475 Published online by Cambridge University Press

SIMPSON, J. E. 1972 Effects of the lower boundary on the head effects of the lower boundary on the head effect of the lower boundary on the head of a gravity current. *J. Fluid Mech.* **53**, 759–768.

WINTERS, K. B., LOMBARD, P. N., RILEY, J. J. & D'ASARO, E. A. 1995 Available potential energy and mixing in density-stratified fluids. *J. Fluid Mech.* **289**, 115–128.

https://doi.org/10.1017/jfm.2013.475 Published online by Cambridge University Press